On the behaviour of body-centred cubic metals to one-dimensional shock loading

J. C. F. Millett · N. K. Bourne · N. T. Park ·
G. Whiteman · G. T. Gray III

Abstract The response of metallic materials to shock loading, like all loading regimes, is controlled largely by factors operating at the microscopic or atomic levels. Over the past few years, face-centred cubic (fcc) metals have received a level of attention where the role of features such as stacking fault energy and precipitation hardening have been investigated. We now turn our attention to body-centred cubic (bcc) metals. In the past, only tantalum, tungsten, and their alloys have received significant attention at high strain-rate conditions due to their use by the ordnance community. In particular, this investigation examines the shear strength of these materials at shock loading conditions. Previous results on tantalum, tungsten, and a tungsten heavy alloy are reviewed, and more recent experiments on niobium, molybdenum, and Ta–2.5 wt% W presented. Results are discussed in terms of known deformation mechanisms and variations of Peierl's stress.

Introduction

The response of materials to high-rate impact loading is of interest to a number of communities. Traditionally, the largest driver has been the military, in it's need to understand armours and their resistance to ballistic attack, but more recently, industries such as the automotive (crashworthiness), aerospace (foreign object damage, bird strike etc.), and satellite protection (orbital debris) have all

J. C. F. Millett (✉) · N. K. Bourne · N. T. Park · G. Whiteman
AWE, Aldermaston, Reading RG7 4PR, United Kingdom
e-mail: Jeremy.Millett@awe.co.uk

G. T. Gray III
MST-8, Los Alamos National Laboratory, Los Alamos,
NM 87545, USA

appreciated the necessity of such information. Unfortunately, a real impact event involves a projectile of arbitrary material, impact velocity, and impact angle onto a target of complex geometry (for example, a fan blade in a jet engine), thus rendering quantitative analysis of the material response extremely difficult or even impossible. Therefore, simpler loading conditions, where the states of stress and strain are completely understood, are employed. At low and intermediate strain-rates, conditions of uniaxial stress (tension or compression) or plane strain (fracture toughness) can be imposed. As strain-rate increases, inertial confinement renders this impossible, and hence conditions of one-dimensional strain dominate, where all strain (ε) is imposed along the impact axis (x), and a three dimensional state of stress (σ) exists, thus,

$$\varepsilon_x \neq \varepsilon_y = \varepsilon_z = 0 \quad \text{and} \quad \sigma_x \neq \sigma_y = \sigma_z \neq 0 \qquad (1)$$

and the axes y and z are orthogonal to x. Such conditions can be generated either explosively via plane wave lenses or by plate impact, where an accurately machined flyer plate of a known material is impacted onto an equally accurately machined target plate, with the flyer driven either by a powder or gas gun. As such, extremely high stresses and pressures are generated, which can be separated into hydrostatic (P is the pressure) and deviatoric (τ is the shear strength) components,

$$\sigma_x = P + \frac{4}{3}\tau \qquad (2)$$

In the weak shock regime (<20 GPa), the shear strength forms a significant part of the overall shock stress, and is an important parameter as it controls the resistance to ballistic attack in armour materials [1]. Therefore, a number of researchers have used various methods to determine this value. The simplest is simply subtracting the hydrostatic

pressure from the impact stress (σ_x), see, for example, the study of Dandekar and Weisgerber [2] in tungsten heavy alloys (WHAs). However, this relies on knowledge of the hydrostatic pressure, which is generally interpolated from ambient pressure bulk modulus data. Therefore, it can be seen that significant errors could be introduced. An alternative method is that of inclined impact (or pressure shear). This method places a thin layer of the target material between two elastic anvils, with an impactor made from the same material as the anvils. Longitudinal and lateral motions of the rear of the target assembly are monitored using interferometric methods. However, the maximum imposed stress is limited by the Hugoniot elastic limit (HEL) of the anvils, and more importantly, the thickness of the sample foil (Duprey and Clifton [3], for example, quote values of 25–127 μm in tantalum) raises questions as to whether these tests actually represent the bulk response of the material in question. Asay and his colleagues [4, 5] compare load–unload to load–reload experiments, monitoring the motion of the interface between the specimen material and a window material (usually single crystal lithium fluoride or sapphire). This method assumes that the target is isotropic and hardens kinematically. As the shock progresses, the impedances of the target and window also change, which can also be a potential source of error. Finally, it is also possible to determine the shear strength via the use of suitably oriented stress gauges. By assuming that the hydrostatic pressure is the average of all three components of stress, then, in combination with equation [2], it is possible to write an equation for shear strength in terms of the longitudinal and lateral stresses, thus,

$$2\tau = \sigma_x - \sigma_y \tag{3}$$

This also assumes that the material is behaving isotropically. The fact that the target has to be sectioned such that a stress gauge can be introduced has also caused others [6] to suggest that the gauge layer perturbs material flow sufficiently that a true in-material state is never reached. However, comparison of shear strength data in tungsten and its alloys (see in the "Results and Discussion" sections) indicate that the gauge method is reliable [7, 8]. A major advantage of lateral stress gauges is that by placing them in the material flow, it is possible to monitor temporal changes in shear strength. In pure nickel [9], we have shown that the shear strength increases over a period of ca. 0.5 μs before reaching a near constant level. This is consistent with the microstructural observations of Murr and Kuhlmann-Wilsdorf [10] who showed that the shock-induced dislocation cell structure only stabilized between 0.5 and 1 μs. In this article, we use this gauging technique to examine the response of body-centred cubic (bcc) materials, tungsten and tantalum and their second period

analogues niobium and molybdenum, and compare the results to previous microstructural observations.

Experimental

All shock loading experiments in this article were performed using 50 mm bore, 5 m long single stage gas guns [11, 12]. Samples of WHA [7], tantalum [13], pure tungsten [8], niobium, molybdenum, and Ta–2.5 wt% W, of thicknesses 10–12 mm and diameters 75 mm (WHA, Nb, and Mo), 45 × 45 mm (tantalum, tungsten) or 60 × 60 mm (Ta–2.5 wt% W) were sectioned in half and a manganin stress gauge (MicroMeasurements J2M-SS-580SF-025) were introduced either 2 mm (tantalum, WHA and Ta–2.5 W) or 4 mm (tungsten, niobium and molybdenum) from the front surface of the specimen. The targets were reassembled using a slow setting epoxy adhesive, with 25 μm of mylar either side of the gauge to electrically insulate it. Gauge data were reduced to lateral stress using the methods of Rosenberg and Partom [14] with a modified analysis that does not require prior knowledge of the impact conditions [15]. Finally, at very low stresses it has also been shown that the geometry of the gauge affects its output, and hence must be accounted for [16]. In the case of the experiments on tungsten, niobium, and molybdenum, a longitudinal stress gauge (MicroMeasurements LM-SS-125CH-048) was supported on the front of the target assembly with a 1 mm cover plate of either dural (aluminium alloy 6082-T6) or copper, matched to the material of the flyer plate. In this way, the gauge would record the longitudinal (impact) stress that the material would experience internally. Gauge calibrations were according to Rosenberg et al. [17]. Using impedance matching techniques, the particle velocity (u_p—as governed by momentum transfer) could be determined, and hence the shock-induced equation of state (Hugoniot) over the impact conditions under investigation could be found. A schematic of the target assembly and gauge placement is shown in Fig. 1.
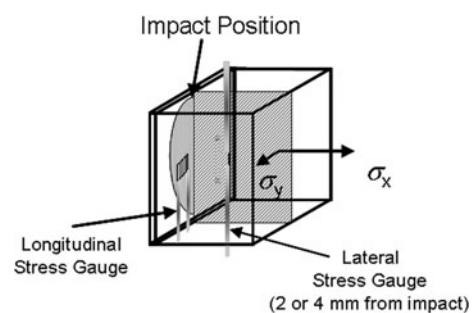

Fig. 1 Specimen geometry

Material data

The acoustic properties of each material were measured using 5 MHz quartz transducers with a Panametrics PR5052 pulse generator, are presented in Tables 1 and 2.

The tantalum used in this study had a near continuous γ fibre (<111>//ND) texture with the α <111> component approximately eight times random. The pure tungsten was manufactured by warm forging of a pressed and sintered powder metallurgy billet. More details can be found in the relevant references [13, 18]. Ta–2.5 W was cold rolled from ca. 300 to 11 mm in a number of stages, with an intermediate annealing treatment of 1100 °C for 1 h between rolling passes. Niobium and molybdenum were received as hot forged 75-mm diameter billets although the conditions were not specified by the manufacturers, followed by a stress relief treatment (Nb—950–1050 °C for 70 min; Mo—900 °C for 30 min). In the case of molybdenum, the {110} and {111} planes were aligned to the bar stock normal (approximately eight times random) whilst in the niobium, there was a strong preference for the {110} planes (approximately 16 times random) to the bar stock normal. No comments can be made concerning the WHA in this study as it was received as a proprietary composition. However, as it was made via a liquid phase sintering route, we have assumed it is largely isotropic. Representative microstructures of tantalum, Ta–2.5 W, tungsten, niobium, and molybdenum are shown in Fig. 2.

Both tantalum and Ta–2.5 W have a largely recrystallised, equiaxed microstructure. The pure tungsten has a somewhat elongated microstructure due to forging below the recrystallisation temperature. The niobium appears to have a high dislocation density, whilst in contrast, the molybdenum dislocation density is low.

In Fig. 3, we present the shock-induced equation of state, the Hugoniot for the base elements involved in this study. Data points are plotted in stress–particle velocity (u_p—velocity of material flow behind the shock front due to momentum transfer) space, with the curve fits showing the hydrodynamic pressure (P_{HD}), according to,

$$P_{HD} = \rho_0(c_0 + Su_p) \tag{4}$$

where ρ_0 is the ambient density and c_0 and S are the shock parameters.

We have included this information as it serves as baseline data that inform the subsequent results in this manuscript.

Results

Typical lateral stress gauge traces for each of the six materials under discussion are shown in Fig. 4. For the sake of clarity, we have split the figure into two, with (a) showing results from tungsten and tantalum alloys, and (b) showing the response of niobium and molybdenum.

Table 1 Acoustic properties and shock parameters of the materials under investigation

	c_L (mm μs^{-1})	c_S (mm μs^{-1})	ρ_0 (g cm^{-3})	v	c_0 (mm μs^{-1})[a]	S[a]
Tantalum	4.13 ± 0.03	2.04 ± 0.03	16.58 ± 0.01	0.339	3.43	1.19
Tungsten	5.22 ± 0.03	2.89 ± 0.03	19.18 ± 0.01	0.279	4.04	1.23
WHA	5.21 ± 0.03	2.85 ± 0.03	17.67 ± 0.01	0.286	4.04[b]	1.23[b]
Niobium	5.11 ± 0.03	2.06 ± 0.03	8.56 ± 0.01	0.403	4.46	1.20
Molybdenum	6.48 ± 0.03	3.49 ± 0.03	10.15 ± 0.01	0.296	5.14	1.22
Ta–2.5 W [32]	4.12 ± 0.03	2.11 ± 0.03	16.78 ± 0.01	0.322	3.32[c]	0.98[c]

c_L, c_S is the longitudinal and shear sound speeds; ρ_0 is the ambient density; v is the Poisson's ratio; c_0 and S are the shock parameters

[a] From Marsh [33]; [b] Assumed to be the same as for pure tungsten; [c] Measured independently and reported in [18]

Table 2 Composition of metals and alloys under investigation

	C	Hf	Fe	Nb	Mo	Ni	Si	Ta	W	Zr	H	N	O
Ta	10		5	25				Bal	25		5	10	50
Ta–2.5 W	<10		0.249		2.933	0.022	0.064	Bal	2.48%		<5	<10	24
W	20										<20	<10	20
WHA	Proprietary composition												
Nb	100	100	14	Bal.	50	14	30	800	100	100	10	40	30
Mo	40		80		Bal.	30	70					12	60

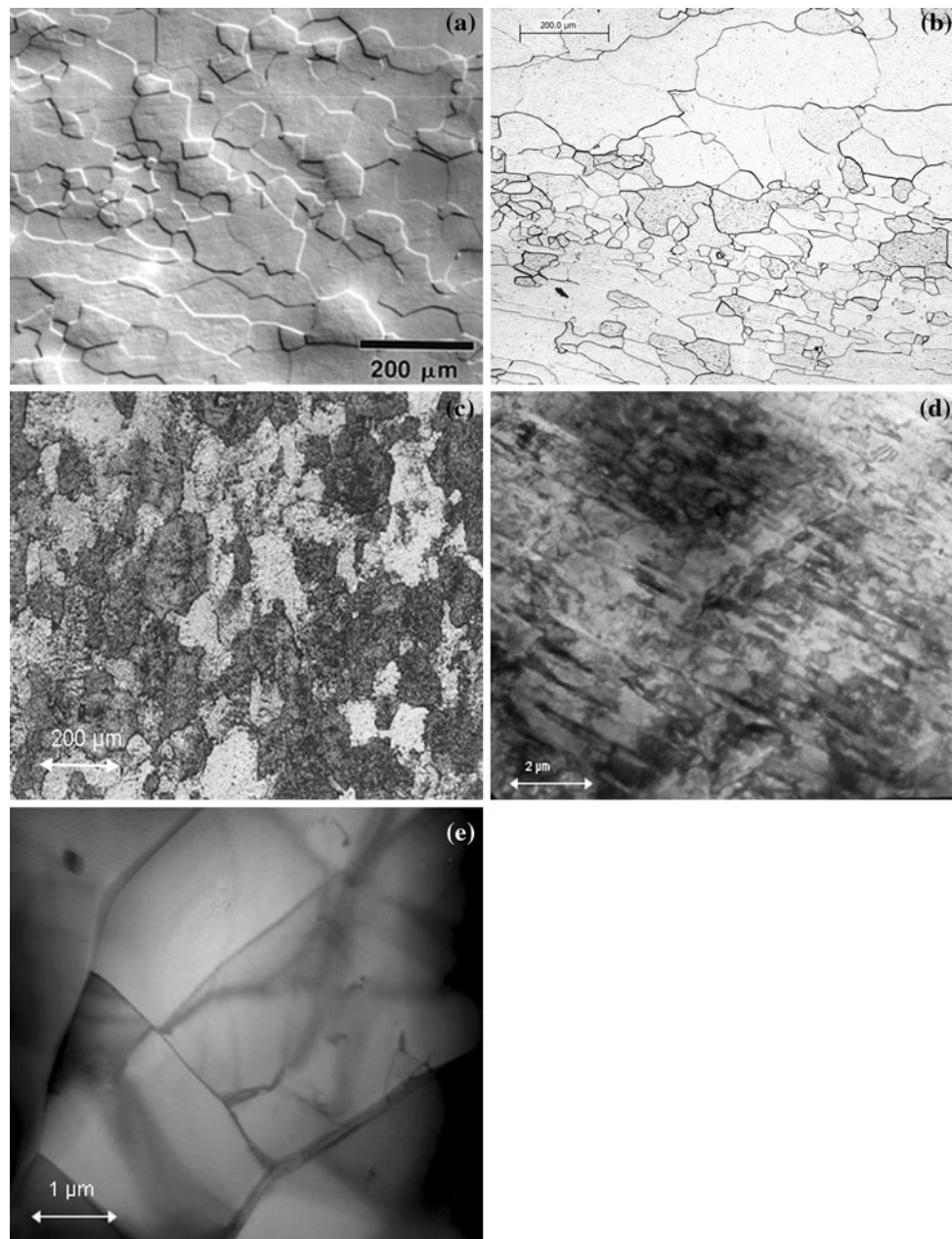Concentrations are in ppm unless otherwise stated

Fig. 2 Microstructures in the as-received state. (**a–c** is optical; **d** and **e** are transmission electron microscopy). **a** Pure tantalum; **b** Ta–2.5 W; **c** Tungsten; **d** Niobium; **e** Molybdenum

Looking at the behaviour of tungsten and tantalum (and the two alloys), it can be seen that there is a commonality in the lateral stress response. Lateral stress rises rapidly as the shock front passes over the gauge location, after which it rises more slowly behind the shock front. From Eq. 3, and assuming that longitudinal stress remains constant, this suggests that shear strength decreases behind the shock front. However, the situation with niobium and molybdenum is significantly different. From the lateral stress histories, it can be seen that lateral stress itself, and hence shear strength are near constant. Therefore, this is a first

indication that different deformation mechanisms are in operation.

Shear strengths have been determined from Fig. 4, using the lateral stress *immediately* behind the shock front, in combination with the known impact stress and calculated via Eq. 3. The results are presented in Fig. 5. Each alloy system and the data for niobium and molybdenum have been plotted separately to aid clarity. In the case of tungsten and its alloys, we have also plotted data from Dandekar and Weisgerber [2], and Zhou and Clifton [19] for comparison purposes. Note that these data from the
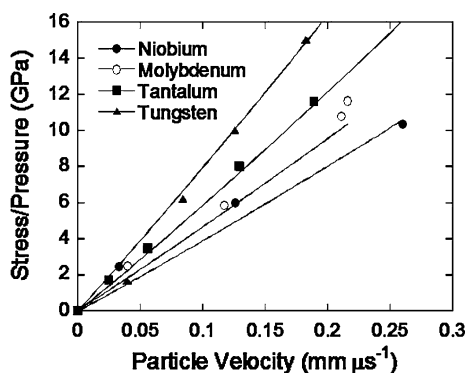
Fig. 3 Hugoniots of the BCC metals in this investigation

literature were gathered using techniques other than lateral gauges. It should be pointed out that these data sets were obtained over a range of WHA compositions. Even so, it

can be seen that there is close agreement between all sets of data, although it appears that pure tungsten at higher stresses is stronger than the WHAs. The shear strengths tantalum and Ta–2.5 W appear broadly similar, with perhaps the alloy being stronger at higher impact stresses. In the case of molybdenum, we have also included a data point calculated by Tonks [20], where again, close agreement with our own data can be observed.

Discussion

The purpose of the study discussed in this article is to expand the existing knowledge of bcc metals. Previous investigations on tungsten alloys and pure tantalum [7, 8, 13] all suggest a common response; namely, in terms of

Fig. 4 Representative lateral stress histories from six bcc metals and alloys. **a** Tungsten, tantalum and alloys. **b** Niobium and molybdenum. Note that longitudinal stress histories have been included
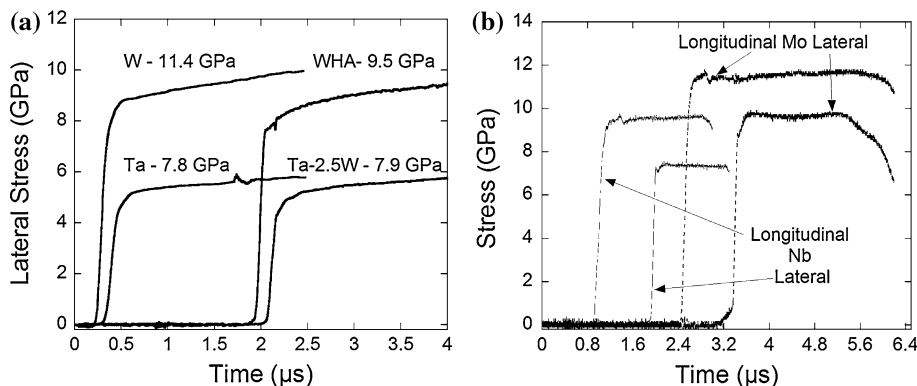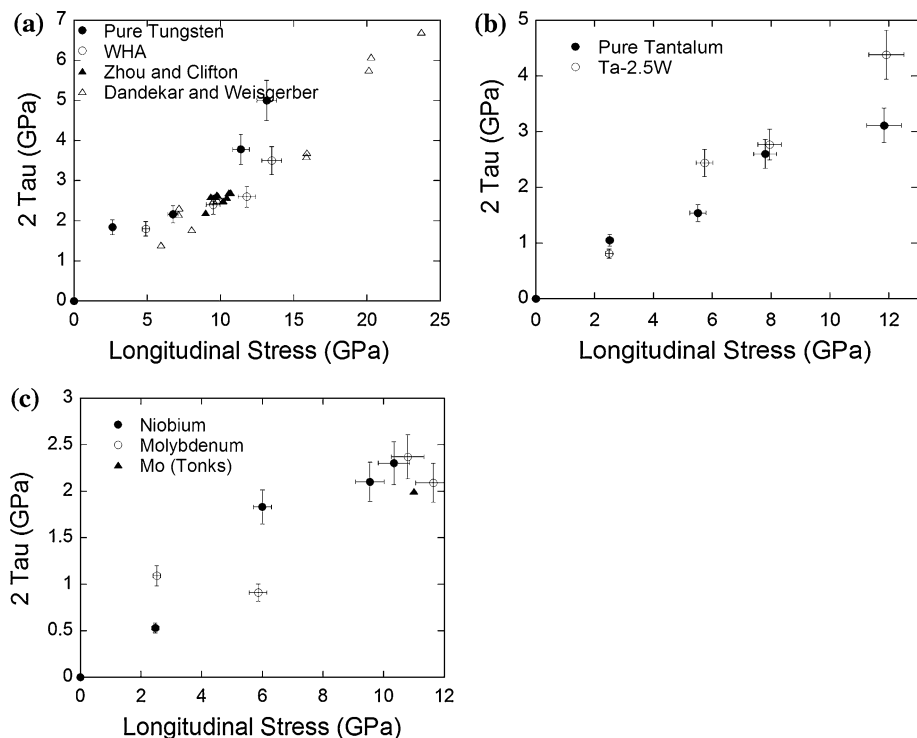

Fig. 5 Shear strengths in bcc metals. **a** Tungsten and alloys. **b** Tantalum and Ta–2.5% W. **c** Niobium and Molybdenum

lateral stress, an observed increase behind the shock front suggests a corresponding *decrease* in shear strength. A hypothesis was advanced [21] that this might be considered a typical bcc response to shock loading. Therefore, such experiments have been extended to niobium and molybdenum (as second period transition element analogues of tantalum and tungsten), and Ta–2.5 W to investigate the effects of simple alloying. To do so, we have chosen to measure lateral stress, using a suitably orientated manganin stress gauge placed in a sectioned sample of the material of interest. However, in doing so, we acknowledge that this is an invasive procedure, in that the gauge is now in a layer of epoxy resin *ca.* 100 μm thick, raising questions about the validity of the technique. Modelling study by Winter and Harris [6] has suggested that the gauge response is dominated by the epoxy layer surrounding it. Therefore, to answer this question, it would be desirable to measure shear strength in a single material, preferably from a single batch, using a variety of techniques. To the authors' knowledge this has not been done. However, from Fig. 5a, it can be seen that the results for WHA, gathered by ourselves using lateral stress gauges [7], via pressure shear [19] and the calculated difference between the Hugoniot and hydrostatic pressure [2], show close agreement, especially since these were from several WHA compositions. Therefore, this figure gives confidence in the validity of the lateral gauge technique and hence we can use it in the analysis of the shock response of other materials. Note that the measured shear strengths for pure tungsten above an impact stress of *ca.* 10 GPa are significantly above those for WHA, indicating that pure tungsten is the stronger material. A likely answer lies in the microstructure. Pure tungsten is of course in a single phase, polycrystalline state, whilst WHA can be considered to be a composite of tungsten grains surrounded by an austenitic face-centred cubic (fcc) layer of lower melting point transition metals (generally iron, nickel, cobalt etc.). Such alloying has a strong influence on the ability of these materials to accommodate plastic deformation at quasi-static strain-rates, and hence it is likely that similar effects occur during shock loading. The HEL of pure tungsten has been placed in the range 3.1–4.4 GPa [4] whilst those of WHAs are lower (1.15–2.76 GPa [2, 22]). It has also been reported by Zhou and Clifton [19] that WHAs show a greater propensity to shear band compared to pure tungsten, hence it is not surprising that pure tungsten displays greater strength at higher impact stresses. In the case of tantalum and its alloy Ta–2.5 W (Fig. 5b), it can also be observed that the strength of the alloy is a little higher than that of the pure metal. The most likely cause is the dilute alloying from the tungsten having a small strengthening effect. We would also point out that the calculated shear strength of molybdenum from Tonks [20], using the weak shock analysis of

Wallace [23, 24], calculated at an impact stress of *ca.* 11 GPa shows close agreement with our own results, again giving confidence in the lateral gauge technique.

The main emphasis of this article concerns the evolution of shear strength behind the shock front, as indicated by the shape of the lateral stress histories presented in Fig. 4. Two sets of behaviour have been observed; an increase in lateral stress, and hence a decrease in shear strength behind the shock front in the case of tungsten, tantalum, and their alloys, and a near constant response behind the shock front in the case of niobium and molybdenum. Given that niobium and molybdenum can be considered second period transition element analogues of niobium and tungsten, these variations in behaviour need explanation. In the case of tantalum, an earlier study measuring lateral stress [13] suggested that deformation occurred via the motion of dislocations already present within the microstructure rather than the generation of new dislocation line length. This was due to the high Peierls (lattice friction) stress that inhibits dislocation generation. Therefore, although an initially high shear stress would be needed to move the existing dislocations, since dislocation motion itself can be considered to be a stress relief mechanism, the shear strength itself behind the shock front would reduce. Given the low level of tungsten additions to Ta–2.5 W, it would appear that the same arguments can be applied, especially as microstructural examination of shocked and recovered samples of tantalum and tantalum–tungsten alloys show essentially the same response [25]. In the case of tungsten, recovered samples of shocked material showed little if any dislocation generation [18], again suggesting that the basic microstructural response is the same. However, the same authors also showed that pure tungsten under shock loading conditions is brittle at room temperature, and in a later study [8], it was suggested that brittle failure generated at the shock front may contribute to the observed reduction in shear strength and increase in lateral stress. The fact that the same behaviour has also been observed in a WHA, with a notionally ductile grain boundary layer indicates that the shock response itself is dominated by tungsten, with additional phases having little influence. However, the fact that niobium and molybdenum *do not* behave in this manner reveals that bcc metals have as wide a range of mechanical response to shock loading as do fcc metals and alloys. For example, changes in stacking fault energy (SFE-γ) change the response from rapid strengthening and equilibration behind the shock front in the high γ nickel to a much flatter response in a low γ austenitic stainless steel [9, 26] as deformation shifts from dislocation multiplication to twin formation. In the case of bcc metals and alloys, it has already been suggested that the Peierls stress (τ_{PN}) strongly influences deformation at a microstructural level; hence an examination of this property of the metals

Table 3 Peierls stress for six metals

Metal	G (GPa)	v	b (nm)	τ_{PN} (MPa)
Nb	36.3	0.403	0.330	70
Mo	121.5	0.296	0.315	629
Ta	69.0	0.339	0.331	252
W	160.2	0.279	0.316	940
Ni[a]	81.7	0.315	0.352	85
TaW	74.71	0.322	0.311	315

[a] In the case of fcc nickel, planes are assumed to be {111}

and alloys under investigation would appear to be a worthwhile exercise. These are tabulated below in Table 3 (including a value for nickel for comparison) and calculated through the following relation [27],

$$\tau_{PN} = \frac{2G}{1-v}\mathrm{Exp}\left(\frac{-2\pi w}{b}\right); \quad w = \frac{a}{1-v} \qquad (5)$$

where G is the shear modulus, b is the lattice parameter, a is the interplanar spacing (in bcc lattices this is assumed to be {110}), and w is the dislocation width.

In the case of niobium, the low Peierls stress would suggest that dislocation generation is easier than in other bcc metals, hence negating the reduction in shear strength behind the shock front. Indeed, recovery studies by Huang and Gray [28] on niobium shocked to 6 GPa showed a dense distribution of dislocation tangles, with planar slip bands and some evidence of twinning. It can also be seen from the transmission electron micrograph of the as-received niobium (Fig. 2d) its initial dislocation density was very high, again suggesting that dislocation generation in this case is easier than the other bcc metals discussed in this report. We would therefore suggest that in this particular case, the high starting dislocation density will reduce the ability of the materials to either move existing dislocations or generate fresh ones, leading to a flatter lateral stress response. The situation with molybdenum is not so clear cut. The high Peierls stress would suggest that it should behave in a similar manner to tantalum and tungsten. The fact that it does not suggests that other processes are in operation. Twinning has been observed by a number of workers [29–31], which would suppress any dislocation-based mechanisms, although there appears to be no consensus concerning minimum threshold stresses where these can occur. Mahajan and Bartlett [29] have also shown that a level of pre-straining to increase initial dislocation density, increases the number of potential dislocation sources, and hence increases dislocation generation behind the shock front, again negating the degree of strength reduction. We do not believe that this is the case in the molybdenum in this study as Fig. 2e shows a very low dislocation density before shock loading. Therefore, we

believe the twinning hypothesis to be the more likely. However, in making these judgments concerning Peierls stress, a number of caveats must be made. First, values of shear modulus and Poisson's ratio have been measured for polycrystalline materials, where as these are likely to be orientation dependent. They are also likely to be pressure dependent as well, and hence at present, quoted values of Peierls stress can be only used as order of magnitude values. However, it is believed that they provide a valuable insight into the variation of shock response between bcc metals and alloys.

Conclusions

A series of plate impact experiments have been performed on six bcc metals and alloys. The response has been monitored using stress gauges mounted such that they are sensitive to the lateral component of stress. A range of behaviour has been observed, from a reduction of shear strength behind the shock front, to a more level response. It has been suggested that as Peierls stress reduces, deformation shifts from one controlled by the motion of pre-existing dislocations, resulting in a reduction in strength to one where dislocation multiplication becomes easier (in the case of niobium) and hence this reduction of shear strength behind the shock front is negated. However, the situation with molybdenum is more complex. It has been suggested that the possibility of twinning could reduce the effect of dislocation-based mechanisms. Alternatively, a high initial dislocation density may also provide a higher of dislocation sources, and hence dislocation generation may play a significant role in deformation.

References

1. Meyer LW, Behler FJ, Frank K, Magness LS (1990) In: Proceedings of the 12th international symposium on ballistics, San Antonio, Texas, pp 419–428
2. Dandekar DP, Weisgerber WJ (1999) Int J Plast 15:1291
3. Duprey KE, Clifton RJ (1998) In: Schmidt SC, Dandekar DP, Forbes JW (eds) Shock compression of condensed matter-1997. AIP Press, Woodbury, p 475
4. Asay JR, Chhabildas LC, Dandekar DP (1980) J Appl Phys 51:4774
5. Lipkin J, Asay JR (1977) J Appl Phys 48:182

6. Winter RE, Harris EJ (2008) J Phys D Appl Phys 41:035503
7. Millett JCF, Bourne NK, Rosenberg Z, Field JE (1999) J Appl Phys 86:6707
8. Millett JCF, Gray GT III, Bourne NK (2007) J Appl Phys 101:033520
9. Millett JCF, Bourne NK, Gray GT III (2008) Metall Mater Trans A 39:322
10. Murr LE, Kuhlmann-Wilsdorf D (1978) Acta Metall 26:847
11. Bourne NK, Rosenberg Z, Johnson DJ, Field JE, Timbs AE, Flaxman RP (1995) Meas Sci Technol 6:1462
12. Bourne NK (2003) Meas Sci Technol 14:273
13. Gray GT III, Bourne NK, Millett JCF (2003) J Appl Phys 94:6430
14. Rosenberg Z, Partom Y (1985) J Appl Phys 58:3072
15. Millett JCF, Bourne NK, Rosenberg Z (1996) J Phys D Appl Phys 29:2466
16. Rosenberg Z, Bourne NK, Millett JCF (2007) Meas Sci Technol 18:1843
17. Rosenberg Z, Yaziv D, Partom Y (1980) J Appl Phys 51:3702
18. Lassila DH, Gray GT III (1994) J Phys IV 4:349
19. Zhou M, Clifton RJ (1997) J Appl Mech 64:487
20. Tonks DL (1996) In: Schmidt SC, Tao WC (eds) Shock compression of condensed matter-1995. AIP Press, Woodbury, p 507
21. Bourne NK, Gray GT III, Millett JCF (2009) J Appl Phys 106:091301
22. Gaeta PJ, Dandekar DP (1988) In: Schmidt SC, Holmes NC (eds) Shock compression of condensed matter 1987. Elsevier, Monterey, p 269
23. Wallace DC (1980) Phys Rev B 22:1477
24. Wallace DC (1980) Phys Rev B 22:1487
25. Gray GT III, Vecchio KS (1995) Metall Mater Trans A 26:2555
26. Millett JCF, Whiteman G, Bourne NK (2009) J Appl Phys 105:033515
27. Smallman RE (1985) Modern physical metallurgy. Butterworths, London
28. Huang JC, Gray GT III (1988) Mater Sci Eng A 103:241
29. Mahajan S, Bartlett AF (1971) Acta Metall 19:1111
30. Wongwiwat K, Murr LE (1978) Mater Sci Eng 35:273
31. Murr LE, Inal OT, Morales AA (1976) Acta Metall 24:261
32. Cotton M (2010) Int J Impact Eng. In submission
33. Marsh SP (1980) LASL shock Hugoniot data. University of California Press, Los Angeles